

Ceramics, Oxides, Geomaterials

LBP.MS.P05

In-situ TEM investigation on lead-free $(\text{Bi}_{1/2}\text{Na}_{1/2})\text{TiO}_3\text{-xSrTiO}_3$

M. Scherrer¹, L.A. Schmitt¹, M. Acosta¹, W. Jo¹, J. Rödel¹, H.-J. Kleebe¹

¹TU Darmstadt - Geomaterial Science, Darmstadt, Germany

$(\text{Bi}_{1/2}\text{Na}_{1/2})\text{TiO}_3$ (BNT)-based ceramics are promising candidates for actuator applications. Prospective and environment-friendly applicability of lead-free materials coupled with strong piezoelectric properties caused a progressive research in the last decades. Common drawbacks of BNT such as large coercive fields (~ 7 kV/mm) [1] are counteracted by the formation of solid solutions. This work focuses on the ergodic relaxor $(1-x)\text{BNT-xSrTiO}_3$ (BNT-xST) which is characterized by relatively high strains at reduced fields ($\sim 0.2\%$ at 4 kV/mm) and the requirement of low poling fields (~ 3 kV/mm).

Previous bulk studies covering the full compositional range of BNT-xST [1, 2] evidenced a maximum in strain at $x = 0.25$. As an incipient piezoceramic it attains enhanced piezoelectric properties (increased piezoelectric coefficient d_{33} and electromechanical coupling factor k_{33}) only upon electrical loading. The electric-field induced phase transition (EFPT) is rationalized to occur in a gradual manner at a fixed temperature. Sample compositions were selected to a) coincide the possible MPB ($x = 0.25$) and b) diverge from the latter ($x = 0.1$). However, an adequate correlation of temperature and electric-field dependent microstructure evolution with corresponding bulk analyses still has to be provided.

In this respect microstructure characterization was systematically carried out by conventional TEM including bright field (BF) and dark field (DF) imaging, high-resolution TEM (HR-TEM) and selected area electron diffraction (SAED) followed up by a set of challenging In-situ transmission electron microscopy (in-situ TEM) experiments.

The addition of ST to the base BNT composition leads to a decrease in depolarization (T_d) and Curie temperature (T_c) of the relaxor. Substituting the pseudo-divalent $(\text{Bi,Na})^{2+}$ by the smaller sized cation Sr^{2+} on the A-site of the general ABX_3 perovskite cell destabilizes the ferroelectric order of BNT. This observation is manifested in the prevalent core-shell structures as depicted in BF fig. 1a and 2a and rationalized consistently by energy-dispersive X-Ray analysis (EDX) and scanning transmission electron microscopy (STEM) techniques which indicate a clear Sr-depletion in the domain-contrasted core regions. For the corresponding DF images in fig. 2b and 2c the outlined superstructure reflection $\frac{1}{2}\{00e\}$ and $\frac{1}{2}\{00o\}$ (o and e resemble odd and even hkl indices, respectively) in fig. 1b were utilized. These reflections are either induced by in-phase (here: $a^0a^0c^+$) or anti-phase (here: $a^-a^-a^-$) octahedral tilting as given in Howard and Stoke's notation [3] or alternatively by antiparallel cation displacement. Subsequent processing of the obtained SAED patterns allowed for a direct identification of non-cubic lattice distortion in terms of rhombohedral R3c and tetragonal P4/mbm phase coexistence within single grains.

In-situ TEM efforts were undertaken to further improve our understanding of the rhombohedral-tetragonal phase transition (T_{r-t}) within the ferroelectrically-active state under applied electric field. Based on interesting bulk measurement results indicating a change in strain mechanism from an extrinsic to an intrinsic contribution at approximately 80°C - 100°C , the ceramic was additionally examined in the temperature range from room temperature to 150°C in an in-situ heating experiment.

1. W. Krauss, D. Schütz, F. A. Mautner, A. Feteira and K. Reichmann, J. Eur. Ceram. Soc. 30 (2010), p. 1827-1832.
2. Y. Hiruma, Y. Imai, Y. Watanabe, H. Nagata and T. Takenaka, Appl. Phys. Lett. 92 (2008), p. 1-3.
3. C. J. Howard and H. T. Stokes, Acta Cryst. B54 (1998), p. 782.

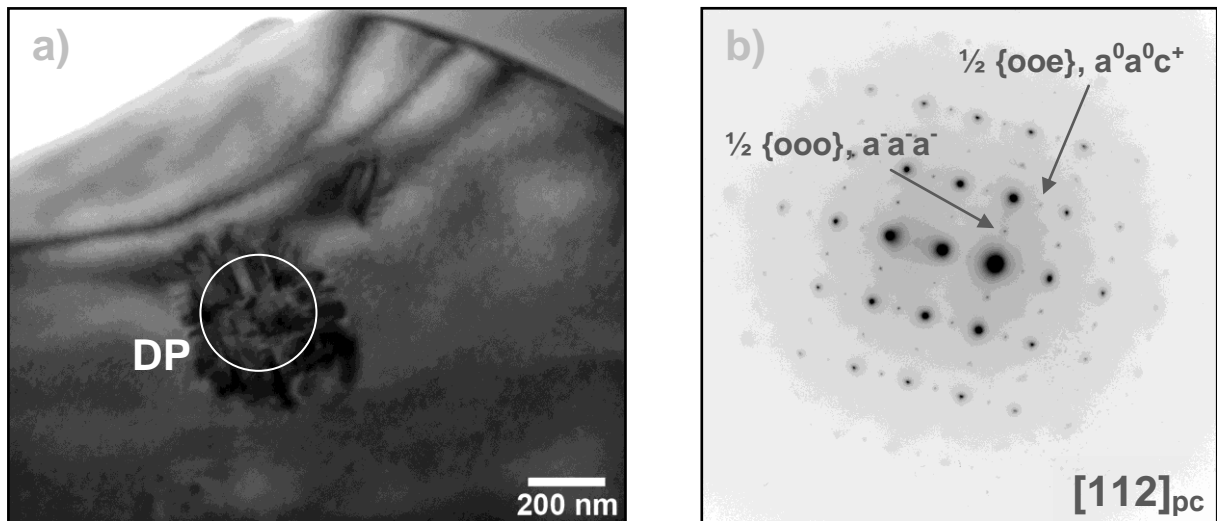


Figure 1. a.) overview bright-field image of the core-shell observed in BNT-25ST. Fig. 1b) corresponding SAED pattern of the investigated grain aligned along $[112]_{pc}$ axis is shown.

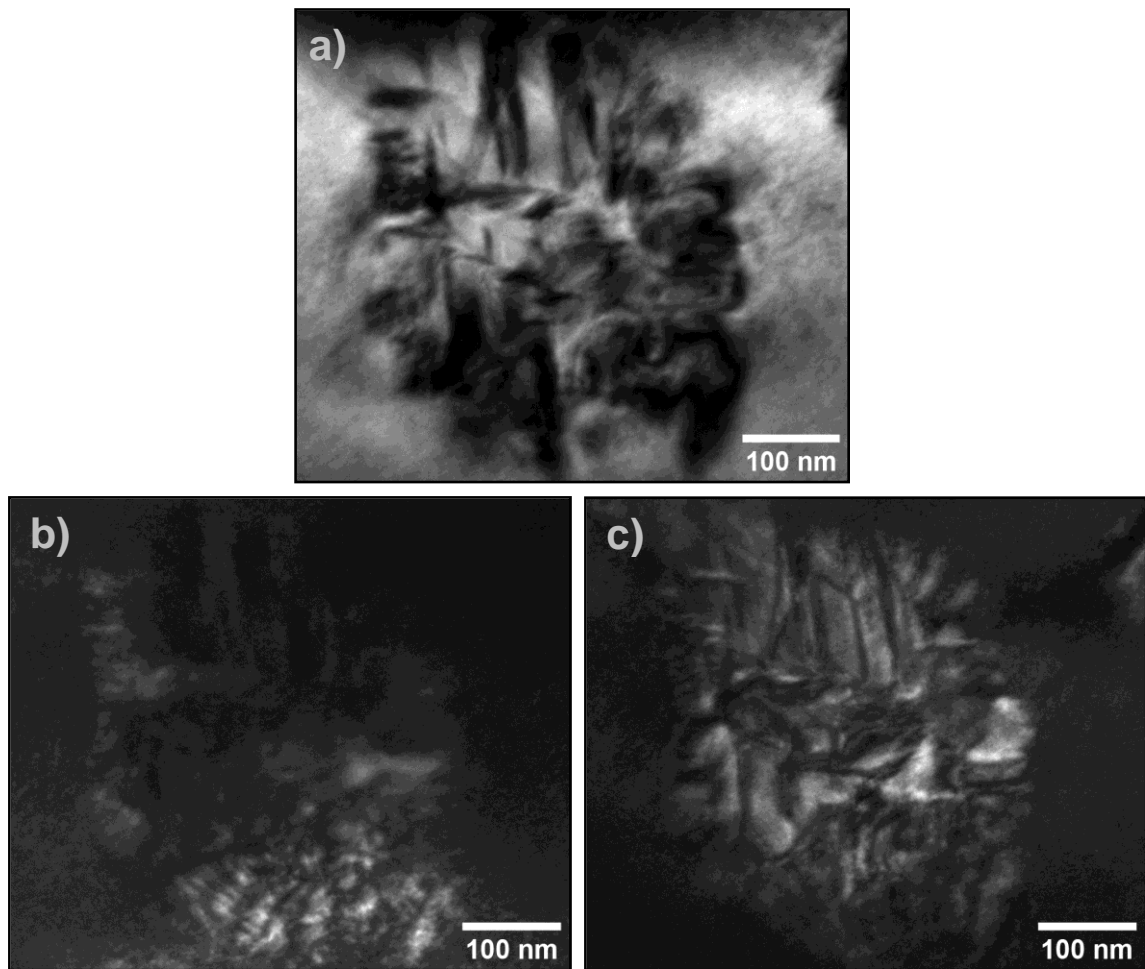


Figure 2. a.) magnified micrograph of a strongly contrasted core region in BF mode. Fig. 2b) & fig. 2c) dedicated DF images employing the above indicated superstructure reflections $\frac{1}{2} \{000\}$ and $\frac{1}{2} \{00e\}$, as outlined in Fig. 1b.